Eur. Phys. J. A **31**, 125–134 (2007)
DOI 10.1140/epja/i2006-10157-x

THE EUROPEAN PHYSICAL JOURNAL A

Regular Article – Hadron Physics

Isotope ratios and isoscaling of spallation products in p(1 GeV) + A reactions

M.N. Andronenko[1], L.N. Andronenko[1], and W. Neubert[2,a]

[1] St. Petersburg Nuclear Physics Institute, Russian Academy of Science, 188300 Gatchina, Russia
[2] Forschungszentrum Rossendorf Inc., 01314 Dresden, Germany

Received: 31 August 2006 / Revised: 15 November 2006
Published online: 10 January 2007 – © Società Italiana di Fisica / Springer-Verlag 2007
Communicated by N. Bianchi

Abstract. An analysis of experimental yields concerning isotopically resolved spallation products from 1 GeV-proton nucleus interactions with targets from Fe to Cs is presented. It was found that the yield ratios of isotopes classified by the difference of the neutron numbers are compatible with relations derived in the grand-canonical approach. The independence of isotope temperatures from the target mass was demonstrated for spallation products. The spallation residues exhibit isoscaling behaviour. The high sensitivity of the isoscaling parameters to the nucleonic composition (N/Z) of the disassembling nuclei is analysed. A unified isoscaling for a common description of similar reactions is discussed.

PACS. 25.40.Sc Spallation reactions

1 Introduction

The phenomenon of isoscaling has been observed in a variety of nuclear collisions followed by statistical fragment production [1–3]. This common behaviour concerns the yield ratio of a specific isotope with nuclear charge Z and neutron number N occurring at the same temperature in two similar reactions that differ only in the isospin asymmetry

$$\frac{Y_2(N,Z)}{Y_1(N,Z)} = C \cdot \exp(\alpha N + \beta Z) \qquad (1)$$

with C as a normalization factor. The isoscaling parameters α and β contain information about the nuclear symmetry energy, chemical potentials and nuclear temperature.

Isoscaling has been established in deep inelastic nucleus-nucleus collisions, multifragmentation and evaporation reactions. Recently, isoscaling behaviour was also observed in nuclear fission [4–6] and for the heavy projectile residues in deep inelastic nucleus-nucleus collisions at 25 A MeV [7,8]. Another promising class of reactions, which has not yet been systematically investigated in terms of isoscaling, pertain to spallation processes. The reaction mechanism is a rather transparent two-step process. The incident light projectile deposits a significant amount of energy while ejecting only a few nucleons well described by the intra-nuclear-cascade (INC) model [9]. Then, the excited nucleus cools down and at adequate low excitation energy between subsequent emissions of nucleons the time should be sufficient for the residual nucleus to reach equilibrium [10]. At the limiting temperature of $T \simeq 4.5$ MeV [11] the mass of the instantaneous residues declines sharply by statistical emission of light and composite particles until a stable nucleus, the observed spallation product, is formed [12]. Actually, this temperature has been established in numerous 1 GeV-proton nucleus interactions [13]. Therefore, one may assume that the remaining spallation residues are products of a statistical process. Consequently, isoscaling should be verifiable.

Spallation should be helpful to confirm recent calculations in the framework of the antisymmetrized molecular-dynamics model (AMD) [14], which predicts an increase of the isoscaling parameters α and β with increased differences in the asymmetry of the two considered reactions. These predictions may be checked by available data which were obtained in hadron-induced reactions using different targets. Furthermore, heavy residues are of high current interest because they allow to extend the range of Z and N to much larger nuclear charges and neutron numbers to test whether a supposed break-down of the isoscaling properties [2,15] will take place or not. In ref. [8] a decrease of the isoscaling parameter α was observed for charges $Z > 28$, *i.e.* for fragments near to the projectile mass, which were produced in very peripheral collisions. Therefore, it is desirable to accomplish systematical studies involving more heavy products formed elsewise.

[a] e-mail: W.Neubert@fzd.de

Table 1. Overview of the used targets.

Targets	Degree of enrichment, %	Consistency
^{54}Fe	99.6	metallic foil
Fe	natural	metallic foil
^{58}Ni	99.7	metallic foil
^{60}Ni	95.0	metallic foil
^{62}Ni	88.0	metallic foil
^{64}Ni	90.0	metallic foil
^{70}Ge	92.0	GeO
^{76}Ge	76.0	GeO
Rb	natural	RbCl
Ag	natural	metallic foil
Cs	natural	CsCl

The yields of such reaction products were measured using a large number of targets bombarded with protons in the energy range from 660 MeV to 12 GeV [16,17]. However, most of the published cross-sections or relative yields were obtained by radiochemical methods and this imposes restrictions on systematic studies.

Here, we have analysed the spallation data [18,19] obtained in p(1 GeV) + A reactions by γ-ray spectroscopy (see sect. 2). The wide variety of these data makes it possible to study isoscaling properties involving not only target combinations different in the neutron number but also such ones with different nuclear charges. Some aspects of isoscaling of these spallation products were already discussed in refs. [20,21] and the present paper is addressed to an extended study and questions related to isoscaling properties. At first (sect. 3) we check up to what extent the available data are consistent with a statistical concept. Thus, we obtain some guidance to analyse the corresponding data. In sect. 4 isoscaling properties of selected target combinations are examined and a unified isoscaling is proposed which allows to represent a wide variety of spallation data in a common description.

2 Data under consideration

The analysis presented here is based on data obtained at the external 1 GeV-proton beam of the PNPI synchrocyclotron in Gatchina. The bulk of these experimental data is published in PNPI internal reports and in the thesis of L.Ch. Batist [18,19]. Since these papers are not available in the public domain we briefly describe specific features of the experiments [18]. The targets (100–200 mg cm^{-2}), mostly consisting of enriched isotopes, were irradiated at the external proton beam with an intensity of $\sim 10^{11}$ protons/s. An overview of the targets is given in table 1.

A pneumatic transport system was used to transport the irradiated targets containing short-lived activities with half-lives $T_{1/2}$ from less than 20 min to some seconds. Activities of longer half-lives were investigated by usual off-line measurements. The γ-ray spectroscopy of these samples was performed with a 20 cm^3 Ge(Li) detector to obtain γ-intensities and therefrom cross-sections. The spallation residues were identified by their characteristic γ-transitions and the respective half-lives. Simultaneous irradiation of Al samples allowed to obtain absolute cross-sections (see tables 2 and 3) using the value $\sigma(1\,\mathrm{GeV}) = 10.6$ mb of the reaction ^{27}Al(p, n3p)^{24}Na. Approximate estimations of cumulative contributions from other nuclei to the extracted nuclide cross-sections do not exceed 10%.

Table 2. Cross-sections of scandium isotopes obtained from various targets at $E_p = 1$ GeV taken from [19]. The numbers given in parantheses are the errors related to the last digit. The errors include statistical errors, inaccuracies of the detector efficiency and the beam monitoring.

Targets	Cross-sections of Sc isotopes, mb				
	^{43}Sc	^{44}Sc	^{46}Sc	^{47}Sc	^{48}Sc
^{54}Fe	8.3(4)	18.3(9)	4.30(25)	0.77(4)	–
^{56}Fe	4.6(3)	16.2(8)	7.8(5)	2.8(2)	0.52(13)
^{58}Ni	6.5(4)	14.5(8)	3.8(3)	0.78(5)	–
^{60}Ni	4.2(3)	12.5(6)	6.2(4)	1.9(1)	0.38(3)
^{62}Ni	3.3(2)	10.0(5)	7.9(5)	3.1(2)	0.66(4)
^{64}Ni	2.6(2)	7.8(4)	8.6(5)	4.5(3)	1.46(9)
^{70}Ge	1.33(8)	4.7(3)	3.6(3)	1.56(9)	0.38(3)
^{76}Ge	0.36(3)	2.00(15)	3.0(3)	2.10(13)	0.84(5)
Rb	0.21(2)	0.91(8)	1.2(1)	0.72(4)	0.22(1)
Ag	0.026(2)	0.120(7)	0.13(1)	0.063(4)	0.020(1)
Cs	0.007(1)	0.042(3)	0.08(1)	0.052(3)	0.021(1)

In addition to the obtained data, spectra of prompt γ-rays emitted from ^{58,60}Ni targets (5–10 g cm^{-2}) were measured by a 50 cm^3 Ge(Li) detector in coincidence with incident protons at lower beam intensities ($\simeq 5 \cdot 10^4$ protons/s) [18]. That way, the identification of short-lived activities could be confirmed and this method made accessible also identification of stable spallation residues. However, in most cases the cross-sections, obtained from these measurements, were found to be considerably lower compared to the values determined by the off-line method. Therefore, in the following analysis we refer in particular to results obtained by the first method previously described.

3 Probe equilibrium for spallation residues

In this section we employ methods used successfully in low-energy nucleus-nucleus collisions and fragmentation reactions, to check the applicability of statistical methods to analyse spallation data. Next, we consider the yield ratios of isotopes which are emitted from the same target.

3.1 Basic concept

A thermally equilibrated system at temperature T, described in the grand-canonical ensemble, can be char-

Table 3. Cross-sections of spallation residues from isotopically separated targets of Ni and Ge at $E_p = 1\,\mathrm{GeV}$ (from [19]). The convention for the errors is the same as in table 2.

Spallation products	Cross-sections of spallation residues from Ni and Ge targets, mb					
	^{58}Ni	^{60}Ni	^{62}Ni	^{64}Ni	^{70}Ge	^{76}Ge
^{20}F	0.39(5)	0.60(8)	0.66(10)	0.60(15)		
^{22}Na	1.13(8)	0.85(7)	0.55(8)	0.36(5)		
^{24}Na	0.93(7)	1.05(7)	1.00(7)	0.97(7)		
^{28}Mg		0.083(15)	0.120(15)	0.160(15)		
^{28}Al	1.7(2)	1.8(2)	1.7(2)	1.25(15)		
^{29}Al	0.57(7)	0.82(9)	0.92(9)	1.2(1)		
^{38}Cl	0.63(6)	0.9(1)	1.1(1)	1.2(1)		
^{39}Cl	0.13(2)	0.28(3)	0.33(3)	0.46(5)		
^{41}Ar	0.15(2)	0.44(4)	0.57(5)	0.82(6)	0.290(15)	0.38(5)
^{38}K	1.2(2)	0.72(15)	0.56(10)	0.36(5)		
^{42}K	2.1(2)	2.7(2)	3.5(3)	4.1(3)	1.66(15)	1.56(15)
^{43}K	0.35(3)	0.70(5)	1.1(1)	1.75(15)	0.48(5)	0.68(6)
^{48}Cr	1.70(15)	0.67(10)	0.35(5)	0.20(5)	0.23(2)	0.04(1)
^{49}Cr	7.3(10)	4.7(5)	2.8(3)	1.7(2)		
^{51}Cr	28.0(25)	24.0(25)	20(2)	14.0(15)	14.7(11)	6.2(5)
^{52}Mn	12.5(8)	9.2(7)	6.5(5)	4.7(4)	7.4(6)	2.70(25)
^{54}Mn	9.0(25)	15.0(15)	18.0(15)	19.0(15)	12.6(14)	9.2(10)
^{56}Mn		1.30(8)	4.5(3)	8.5(5)	1.62(15)	4.2(3)
^{58}Mn			0.43(5)	1.60(15)		
^{52}Fe	1.45(15)	0.33(3)	0.160(13)	0.11(1)		
^{53}Fe	10.0(8)	3.7(3)	1.85(20)	1.10(15)		
^{59}Fe			3.7(3)	9.8(9)	0.72(7)	3.6(3)
^{55}Co	5.6(4)	2.3(2)	1.2(1)	0.75(8)	1.06(10)	0.24(3)
^{56}Co	32(2)	10.0(8)	5.5(4)	3.5(3)	5.5(5)	3.3(3)
^{57}Co	32(2)	29(2)	17.5(15)	10.5(9)	16.4(15)	7.5(7)
^{58}Co		32(2)	17.0(15)	15.0(15)	17.3(15)	11(1)
^{60}Co			21(2)	19(2)	2.1(3)	5.4(6)
^{61}Co			15(2)	15(2)		3.2(8)
^{57}Ni	26.0(17)	1.20(15)	0.6(1)	0.6(1)	0.61(5)	0.16(2)
^{60}Cu					4.0(5)	1.1(1)
^{61}Cu					9.2(10)	2.7(3)
^{65}Zn					30(3)	12.6(13)

acterized by a primary fragment yield $Y(N,Z)$ explicitly given in ref. [22]. The yield *ratio* of two isotopes $(Z, A_1, N_1 = A_1 - Z)$ and $(Z, A_2, N_2 = A_2 - Z)$ of a given fragment follows the relation

$$\mathbf{R} = \left(\frac{N_2 + Z}{N_1 + Z}\right)^{3/2} \cdot \exp\left(-\frac{\varepsilon_2 - \varepsilon_1}{T}\right) \cdot \exp\left(\frac{\mu_n \Delta N}{T}\right) \quad (2)$$

taking into account the convention that $A_2 > A_1$ and $N_2 > N_1$. The corresponding difference of the neutron numbers is $\Delta N = N_2 - N_1$, ε_1, ε_2 are the mass excesses of both isotopes and μ_n is the neutron chemical potential of the system.

In low-energy nucleus-nucleus reactions it was found that the significant ordering parameter in the relative yields of isotopes is the neutron-to-proton ratio of the combined system (c) of target (t) + projectile (pr) rather than that of the target alone [23]. In ref. [24] it was shown that for fixed temperature T the chemical potential μ_n increases also with the neutron-to-proton ratio of the considered ensemble. Provided that the conditions of ref. [25] are satisfied we assume that μ_n is a *linear* function of the

ratio N_c/Z_c,

$$\mu_n = \mu_{no} + \mu'_n \cdot N_c/Z_c \tag{3}$$

with

$$N_c/Z_c = (N_t + N_{pr})/(Z_t + Z_{pr}). \tag{4}$$

Equation (3) can be regarded as the first-order series expansion of the neutron chemical potential at fixed temperature, whereas μ'_n may be interpreted as the intrinsic chemical potential of the combined system.

In the following we consider proton-induced reactions. Then, the ratio N_c/Z_c simplifies to

$$\xi = N_c/Z_c \rightarrow \frac{N_t}{Z_t + 1} \tag{5}$$

and eq. (2) can be written as

$$\mathbf{R} = \left(\frac{N_2 + Z}{N_1 + Z}\right)^{3/2} \cdot \exp\left(-\frac{\varepsilon_2 - \varepsilon_1}{T}\right) \times \exp\left(\frac{\mu_{no}\Delta N}{T}\right) \cdot \exp\left(\frac{\mu'_n}{T}\Delta N \cdot \xi\right). \tag{6}$$

Equation (2) is valid when the isotopes "1" and "2" are produced at the same temperature T. Under this condition, supposed that the difference of the neutron numbers ΔN is fixed, eq. (6) simplifies to

$$\mathbf{R} \propto e^{c_1 \cdot \Delta N} \cdot e^{c_2 \cdot \Delta N \cdot \xi} = C e^{S_{\Delta N} \cdot \xi}, \tag{7}$$

where $c_1 = \mu_{no}/T$, $c_2 = \mu'_n/T$ and $S_{\Delta N} = c_2 \cdot \Delta N$.

In this notation we get

$$\ln(\mathbf{R}) \propto S_{\Delta N} \cdot \xi \tag{8}$$

and the exponential slope is related to the difference of the neutron numbers

$$S_{\Delta N}(\Delta N = 1, 2, 3, 4, 5, \ldots) = c_2 \cdot (1 : 2 : 3 : 4 : 5 \ldots). \tag{9}$$

Equation (7) predicts that all isotopic ratios, specified by fixed ΔN, lie on a line in a semi-log plot *versus* N_c/Z_c or $\xi = N_t/(Z_t + 1)$. Furthermore, the logarithmic slopes $S_{\Delta N}$ derived from data, plotted for isotopic pairs counted among $\Delta N = 2$, are expected to be twice larger than those characterized by $\Delta N = 1$, or generally, as predicted by eq. (9).

These consequences have been verified in low-energy nucleus-nucleus interactions [26,27] and also in proton-induced fragmentation at 1 GeV [20,28]. This means, vice versa, that the assumption about the proportionality of μ_n to the ratio N_c/Z_c is not in contradiction with the experimental data. Therefore, we will show later in sect. 4.3 that the ratio N_c/Z_c is particularly suited for the characterization of the nucleonic composition of each disassembling source.

3.2 Application to spallation data

The yield data concerning different isotopes from spallation reactions, presented in tables 2 and 3, allow an analysis using the above statistical concept. The sum of the measured cross-sections, obtained for a given target, represents about 20% of the total inelastic reaction cross-section estimated in [19] by the relation

$$\sigma_{tot} \simeq 50 \cdot A_t^{2/3}\,(\text{mb}).$$

Yield ratios specified by ΔN were calculated from the production cross-sections of ^{43,44,46,47,48}Sc given in table 2. These data, acquired using targets from Fe to Cs [18], are presented in fig. 1. As long as ΔN is kept fixed, the expected exponential increase of the isotopic ratio $\mathbf{R}$ as a function of $\xi = N_t/(Z_t + 1)$ has been observed. Then each data set presented in fig. 1 was fitted by an exponential form $\mathbf{R} = C \cdot \exp(S_{\Delta N} \cdot \xi)$. Apart from some fluctuations around the fit lines the data agree with an overall logarithmic increase indicating a common temperature. The parameters $S_{\Delta N}$ obtained from these fits are displayed in fig. 2 as a function of ΔN demonstrating the validity $S_{\Delta N} = c_2 \cdot \Delta N$ and generally relation (9). Thus, one may conclude that the spallation products arise from an equilibrated source. In this context we refer to a similar study [28] where fragmentation products with $Z = 2$–5 from 1 GeV p + A collisions were analysed. The ratios of isotope yields specified by ΔN behave very similarly.

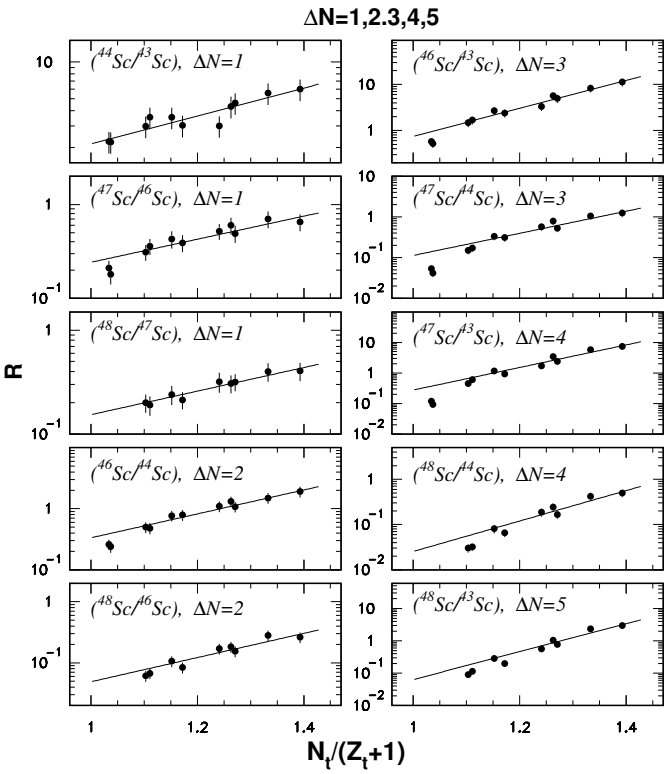

Fig. 1. Yield ratios $\mathbf{R}$ of Sc isotopes obtained in spallation reactions of the target nuclei ^{54,56}Fe, ^{58,60,62,64}Ni, ^{70,76}Ge, Rb, Ag and Cs. The ratios are classified by $\Delta N = 1$, 2, 3, 4, 5. The lines are exponential fits to the experimental points.

3.3 Feature of isotope temperatures

The isotope temperatures [29] provide a further indication that global equilibrium is attained in the reaction under

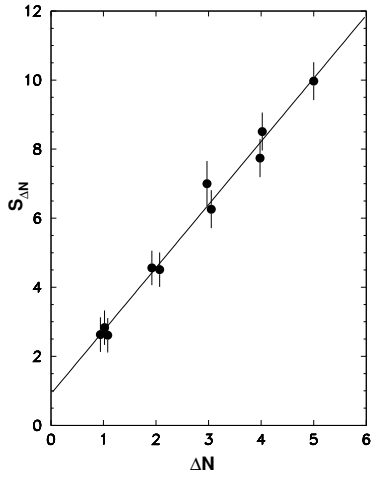

Fig. 2. The slope parameters $S_{\Delta N}$ obtained from exponential fits to the data given in fig. 1 as a function of the difference of the neutron numbers ΔN. The line shows a linear fit to the data points.

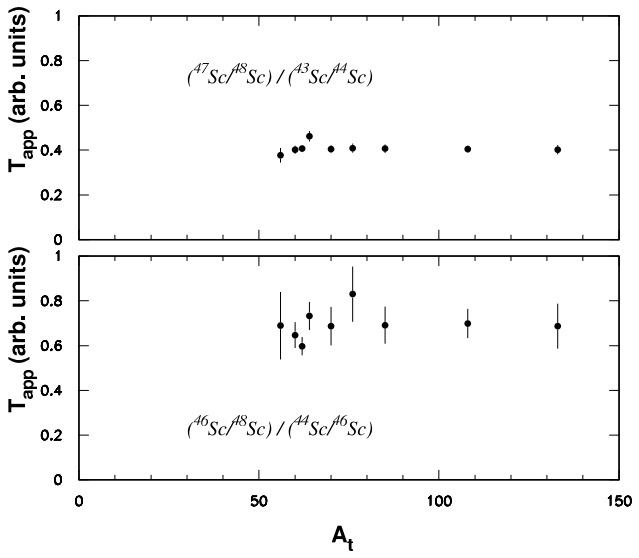

Fig. 3. Noncalibrated isotope temperatures as a function of the target mass derived from scandium spallation products registered in 1 GeV-proton interaction with target nuclei from fig. 1 and table 2.

consideration. Already in ref. [13] it was shown that in proton-induced fragmentation reactions *relative* temperatures can be derived from thermometers constructed by certain double-yield ratios. A striking feature of these relative apparent temperatures is a rather weak dependence on the target mass. Here, we derived in an analog way relative temperatures from specific combinations (see fig. 3) of the spallation products ^{43}Sc, ^{44}Sc, ^{46}Sc, ^{47}Sc and ^{48}Sc. The corresponding relative apparent temperatures plotted in fig. 3 are nearly constant in the target mass range from $A_t = 56$ to $A_t = 133$. Hence, spallation at 1 GeV seems to be characterized by a unique temperature as far as medium-weight targets are considered.

4 Isoscaling behaviour of spallation residues

4.1 Target combination ^{76}Ge/^{70}Ge

The observed properties of the yield ratios of spallation products advocate the adoption of statistical concepts as precondition for isoscaling. As explained in the introduction, this phenomenon is related to the yield ratios Y_2/Y_1 of specific isotopes (N, Z) produced in two similar reactions:

$$\frac{Y_2(N,Z)}{Y_1(N,Z)} \propto \exp\left(\frac{\Delta\mu_n N}{T}\right) \cdot \exp\left(\frac{\Delta\mu_p Z}{T}\right) = C \cdot \exp(\alpha N + \beta Z), \quad (10)$$

where $\Delta\mu_n$ and $\Delta\mu_p$ are the differences of the neutron and proton chemical potentials belonging to the reactions "1" and "2". It is conventionally suggested that the neutron to proton ratio of system "2" is larger than that of system "1" [2]. A common fit of Y_2/Y_1 against N and Z of spallation products allows to determine the parameters $\alpha = \Delta\mu_n/T$ and $\beta = \Delta\mu_p/T$ assuming that the nuclear temperature T in both systems is nearly the same.

In refs. [1,2] it has been shown that the relative isotope yields scaled with the factor $\exp(-\beta Z)$ lie along a straight line on a semi-log plot $(Y_2/Y_1)\exp(-\beta Z)$ as a function of the neutron number N of the reaction products.

The above spallation data allow inspection of isoscaling behaviour for higher Z and N up to neutron numbers $N \leq 33$. Figure 4 demonstrates this behaviour for the residues registered in 1 GeV-proton interactions with the target nuclei ^{70}Ge and ^{76}Ge, ref. [18]. Two examples of individual fits of isotope chains of Sc and Mn are shown (see insert of fig. 4). The obtained parameters α and β were

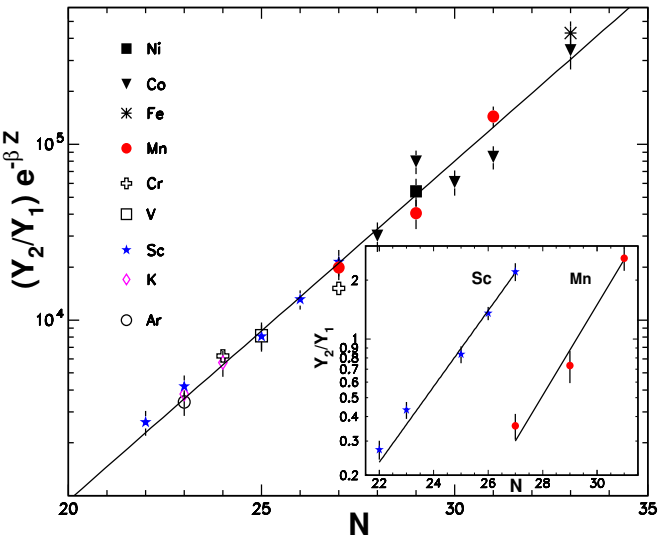

Fig. 4. The scaled yield ratios of spallation products from ^{70}Ge and ^{76}Ge targets plotted as a function of the neutron number N. The data points for isotopes of a given element are displayed by the same symbol (see notation inside of the figure). The solid line is the best fit to the plotted data points obtained with eq. (1).

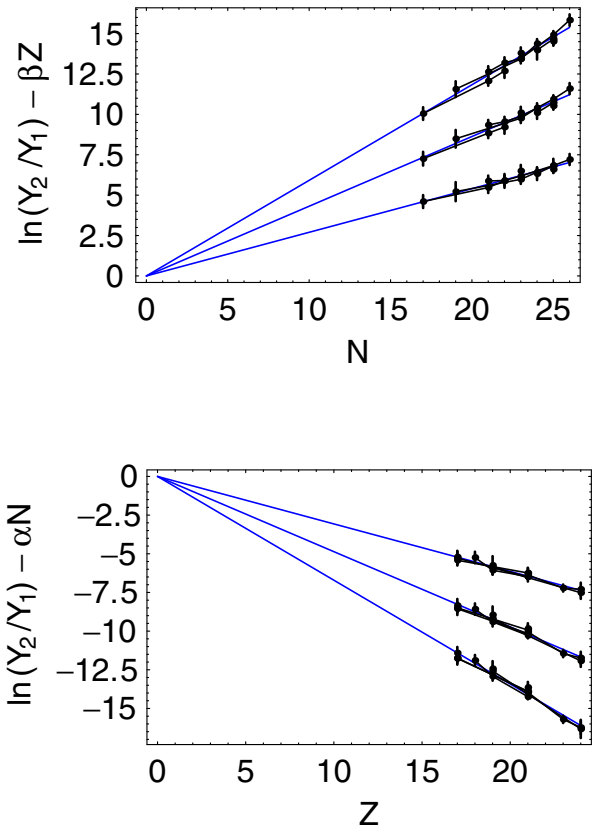

Fig. 5. Scaled yield ratios of spallation products from 1 GeV-proton interactions with Ni targets as a function of the neutron (or proton) numbers of the fragments. Upper panel: isotopic scaling, the lines correspond to the combinations ^{60}Ni/^{58}Ni, ^{62}Ni/^{58}Ni and ^{64}Ni/^{58}Ni (upwards). Lower panel: isotonic scaling, the assignment to the lines is in the opposite direction.

found to be equal to (0.45 ± 0.03) and (-0.46 ± 0.02), respectively. All spallation products displayed in the range $22 \leq N \leq 33$ (see fig. 4) lie near to the line corresponding to the common fit, *i.e.* they show a satisfying isoscaling. The observed deviations are mainly due to uncertainties in the cross-sections.

4.2 Selected combinations of Ni targets

To improve the accuracy of the parameters α and β two selection criteria were applied to spallation products: $Z > 16$ and $A < A_t - 7$. The first criterion was used to reject products of fragmentation and the second one to eliminate some direct processes (like knockout etc.). For example, INC calculations, accomplished for p+Ni interactions [30], showed that at the initial cascade stage, on average, $\simeq 6$ nucleons are lost from the target. This is in agreement with the measured mass loss ΔA at 1 GeV incident energy [31].

Figure 5 shows the scaled yield ratios of spallation products for 3 combinations of Ni targets, ^{60}Ni/^{58}Ni, ^{62}Ni/^{58}Ni and ^{64}Ni/^{58}Ni, which correspond to differences $\Delta N_t = 2, 4, 6$. The striking feature in fig. 5 is that the logarithmic slopes and the corresponding parameters α and β vary for the three studied examples. Already in ref. [15] it was mentioned that α and β are also sensitive to the isospin asymmetry if different combinations of reactions are considered. In order to extract this dependence one has to rule out the influence of other disturbing quantities.

i) For instance, in the grand-canonical ensemble limit of dilute non-interacting particles the parameters α and β are related also to the relative nucleon density when forming the fragments [1]. But that should have little relevance since spallation residues are remnants of an evaporation-like process occurring at normal nuclear density.

ii) In ref. [15] it was pointed out that sequential decays affect minimally or not the isoscaling.

iii) Both parameters α and β are proportional to the reciprocal of the temperature. Therefore, one has to constrain the temperature with experimental information to draw conclusions about the influence of the isospin asymmetry, or generally, the nucleonic composition of the involved reactions. From fig. 3 follows that at 1 GeV-proton energy, the spallation remnants from medium-weight targets can be characterized by nearly the same temperature. The reason of different isoscaling parameters α and β in fig. 5 may hardly be explained by different temperatures. Consequently, the unequal values α (or β) observed for different combinations of reactions in fig. 5 are to be attributed to differences of the nucleonic compositions of the disassembling nuclei.

4.3 Dependence on the nucleonic composition of the emitting sources

In ref. [21] we pointed out the high sensitivity of isoscaling parameters to the nucleonic composition of the emitting sources. Here we consider two approaches to demonstrate the explicit dependence of α and β on the difference of the isospin asymmetries of the sources.

4.3.1 Semiempirical approach

The first approach is based on the experimental findings of the preceding sections and supported by ref. [25]. There, it has been shown that the conservation of the mean mass and charge of the emitting source (denoted by s) within a given volume has the consequence that the chemical potential μ becomes approximately a linear function of the appropriate neutron-to-proton ratios. Therefore, the isoscaling parameters α and β, both proportional to $\Delta\mu_n$ and $\Delta\mu_p$, may be modified by a quantity $\Delta(N/Z)_s = (N/Z)_2 - (N/Z)_1$ for α and for β by $\Delta(Z/N)_s = (Z/N)_2 - (Z/N)_1$, where the indices $i = 1, 2$ are related to the two reactions under consideration. According to relation (5), for proton-induced reactions, one can write:

$$\begin{aligned} \Delta(N/Z)_s &= N_{t2}/(Z_{t2}+1) - N_{t1}/(Z_{t1}+1) \\ \Delta(Z/N)_s &= (Z_{t2}+1)/N_{t2} - (Z_{t1}+1)/N_{t1}\,, \end{aligned} \qquad (11)$$

where N_{t1}, Z_{t1} and N_{t2}, Z_{t2} are the neutron and proton numbers of the targets "1" and "2", respectively. For

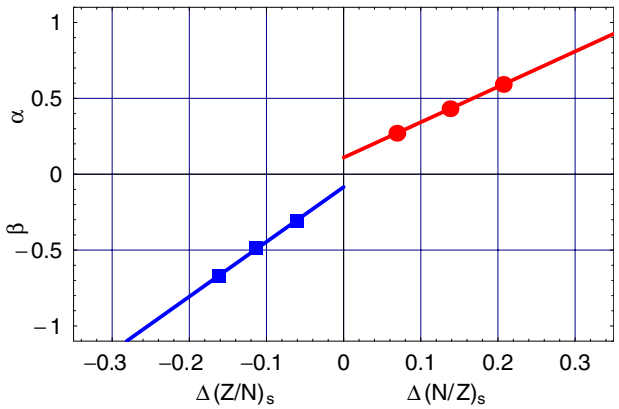

Fig. 6. The isoscaling parameter α (points) as function of the quantity $\Delta(N/Z)_s$ and the parameter β (boxes) *versus* $\Delta(Z/N)_s$ for the 3 combinations plotted in fig. 5. The error bars are less than the size of symbols.

simplicity, we assume here that the neutron-to-proton ratio of each of the emitting sources is approximately the same as in the entire combination, *i.e.* target + proton. This assumption is also supported by recent calculations performed with the INC code [9] for incident energies in the GeV range. Although the masses of the emitting sources differ from those of the targets, the difference of neutron-to-proton ratios of the emitting sources is similar to that of the targets. This was shown for p + ^{112}Sn and p + ^{124}Sn interactions in ref. [9].

The isoscaling parameters α and β derived from fits to the data analysed in sect. 4.2 by using relations (10) are plotted in fig. 6 as functions of quantities defined in eq. (11). The obtained values α (or β) comply with a linear relationship $\alpha \propto \Delta(N/Z)_s$ and $\beta \propto \Delta(Z/N)_s$, respectively.

On this basis we introduce reduced isoscaling parameters α' and β' as follows:

$$\alpha = \alpha' \cdot \Delta(N/Z)_s\,, \qquad \beta = \beta' \cdot \Delta(Z/N)_s\,. \tag{12}$$

As a result, eq. (10) becomes

$$\frac{Y_2}{Y_1} = C \cdot \exp(\alpha' \cdot \Delta(N/Z)_s \cdot N + \beta' \cdot \Delta(Z/N)_s \cdot Z), \tag{13}$$

where the ratio of the isotope yields of the fragments is an explicit function of the nucleonic compositions of the emitting sources. The application of eq. (13) to the data presented in fig. 5 allows to unify the three sets which depict various combinations of Ni isotopes into a common group using the renormalized ordinates with common values for α' and β' for all combinations:

$$\begin{aligned} \alpha' \cdot N &= \Delta(N/Z)_s^{-1}(\ln(Y_2/Y_1) - \ln C - \beta' \Delta(Z/N)_s Z) \\ \beta' \cdot Z &= \Delta(Z/N)_s^{-1}(\ln(Y_2/Y_1) - \ln C - \alpha' \Delta(N/Z)_s N), \end{aligned} \tag{14}$$

as shown in fig. 7.

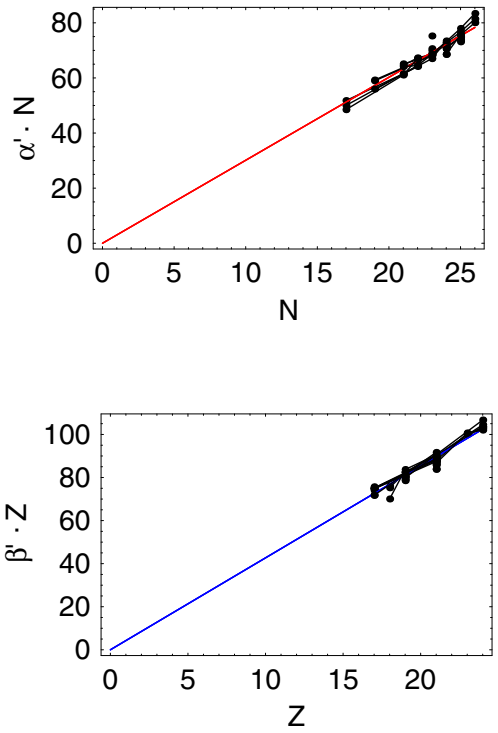

Fig. 7. Unified isotopic and isotonic scaling for three combinations of Ni isotopes plotted in fig. 5 scaled with the factors $\Delta(N/Z)_s^{-1}$ (upper panel) and $\Delta(Z/N)_s^{-1}$ (lower panel), see (14). Here, the error bars shown in fig. 5, were deleted for the clearness of 45 points compressed in one band.

4.3.2 Unified isoscaling

The above findings encourage us to consider not only pairs of reactions with different isospins but also sources with different nuclear charges and various nucleonic compositions [20,21,32]. In order to verify the unified isoscaling[1] as presented by eq. (13) we processed as many data as possible. The fit procedure was applied to 15 combinations of targets including ^{58,60,62,64}Ni and ^{70,76}Ge. One of them, the combination (p+^{62}Ni)/(p+^{70}Ge) having the smallest $\Delta(N/Z)_s = 0.02$, was discarded due to the too large χ^2.

Figure 8 (upper panel) shows the dependence of the obtained parameters α (or β) on $\Delta(N/Z)_s$ or $\Delta(Z/N)_s$, respectively, thus confirming the approach (12). Here we stress nonstatistical deviations of isoscaling parameters in comparison with fig. 6. The fluctuations of the data points in fig. 8 can be related to indeterminations of the neutron-to-proton ratios of the used values regarding $(N/Z)_i$ of the excited nuclei at the decay phase. Thus, the upper panel of fig. 8 illustrates the high sensitivity of isoscaling parameters to the difference of $(N/Z)_s$ of the emitting sources. Assuming a changement of A_t by only one nucleon, it was found that the position of the parameters α is shifted on the axis $\Delta(N/Z)_s$ proportionally to $1/Z_t \sim \pm 0.036$, *i.e.*

[1] We mention that the term "unified isoscaling" has not the same meaning as "generalized isoscaling" in ref. [33], where the isoscaling relationship has been extended to consider two systems at different temperatures.

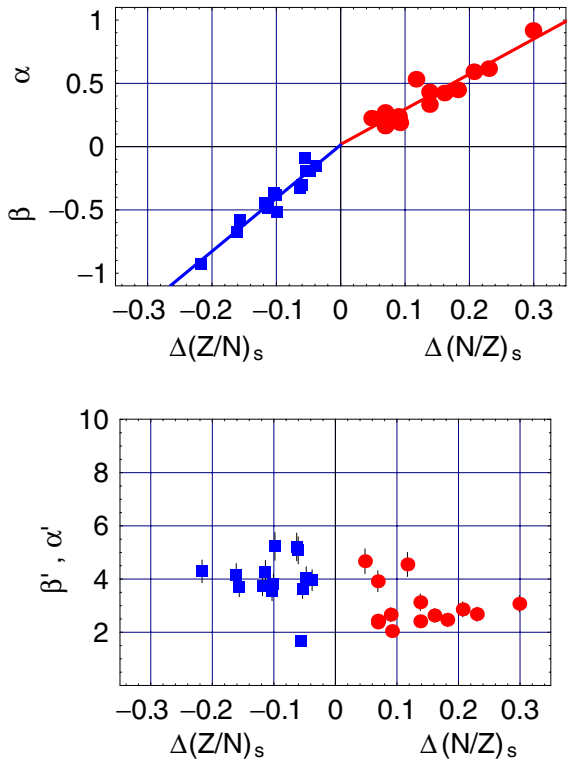

Fig. 8. Upper panel: the isoscaling parameters α and β obtained by eq. (1) for 14 combinations of ^{58,60,62,64}Ni and ^{70,76}Ge as a function of $\Delta(N/Z)_s$ and $\Delta(Z/N)_s$. Lower panel: the reduced isoscaling parameters α' and β' from eqs. (12) for the corresponding combinations.

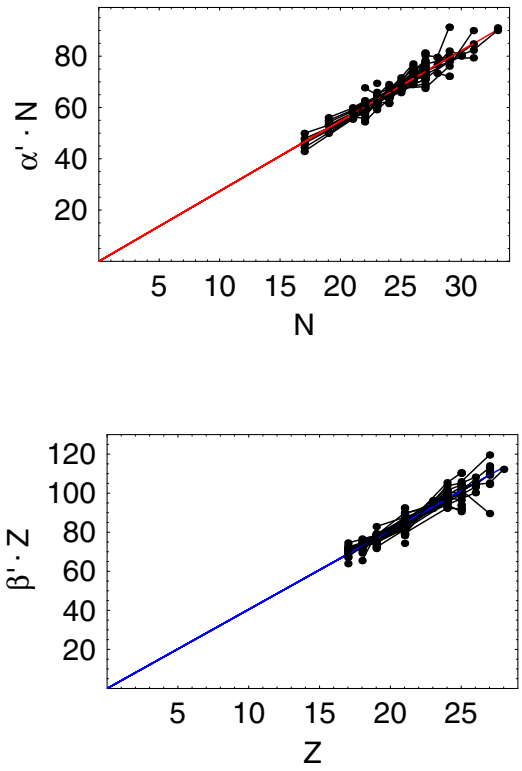

Fig. 9. Unified isoscaling of spallation residues related to 14 combinations of Ni and Ge targets with the mean values of α' and β' presented in fig. 8. The error bars were deleted to depict the slopes of 14 close curves containing 250 data points. Upper panel: unified isotopic scaling. Lower panel: unified isotonic scaling.

remarkably away from the line presenting the fit to the data points. For example, suggesting that A_t of one of the involved Ni targets is in question, then the consideration of unified isoscaling would allow to determine it (see fig. 6).

Whereas the isoscaling parameters α and β vary from one to another combination of targets, the corresponding reduced parameters α' and β' are indeed independent on the difference of the nucleonic compositions as shown in fig. 8 (lower panel). The nearly constant temperatures extending over several target masses (see fig. 3) here are reflected in a similar behaviour of α' and β' derived from spallation products related to target masses from $A_t = 58$ to $A_t = 76$. Therefore, the reduced parameters α' and β' are supposed to be the relevant quantities in the isoscaling relationship and they are dependent on the temperature such as α and β, which is obvious from relations (10) and (12). The yield ratios Y_2/Y_1 of 14 combinations, scaled with the differences of the nucleonic compositions (according to (11)) of the corresponding target pairs applied to relation (14) with common values $\alpha' = 2.7 \pm 0.2$ and $\beta' = 4.1 \pm 0.2$, are shown in fig. 9. More than 250 points are located in a narrow band around the exponential relationship, regardless of the various combinations.

4.3.3 Model-based analysis

In ref. [3] it was pointed out that the isoscaling parameters depend on the asymmetry of the two reactions which leads to a linear relationship between α and $(Z/A)_2^2$ for a fixed reaction denoted by "1". Corresponding relations can be derived in the framework of the expanding emitting source (EES) model [34], the antisymmetrized molecular dynamics (AMD) model [14] and the statistical multifragmentation model [9]. In the grand canonical limit α and β will have the form [35]:

$$\alpha = 4C_{sym}/T \cdot ((Z/A)_1^2 - (Z/A)_2^2),$$
$$\beta = 4C_{sym}/T \cdot ((N/A)_1^2 - (N/A)_2^2), \qquad (15)$$

where $(Z/A)_i^2$ and $(N/A)_i^2$ $(i = 1, 2)$ are the squares of Z or N over A for reactions "1" and "2", respectively, and C_{sym} is the coefficient of the symmetry term of the nuclear binding energy. C_{sym} provides the dominant contribution to the difference of the separation energies (or chemical potentials) in systems of comparable mass and excitation energy [3] thus modifying the isoscaling parameters.

On the basis of eqs. (15) the isoscaling parameters α and β can be factorized as in relations (12):

$$\alpha = \alpha'_m \cdot \Delta(Z/A)_s^2\,, \qquad \beta = \beta'_m \cdot \Delta(N/A)_s^2 \qquad (16)$$

with

$$\alpha'_m = \beta'_m = 4C_{sym}/T. \qquad (17)$$

Here, we approximate also the nucleonic composition of the emitting source (s) by the corresponding one of the

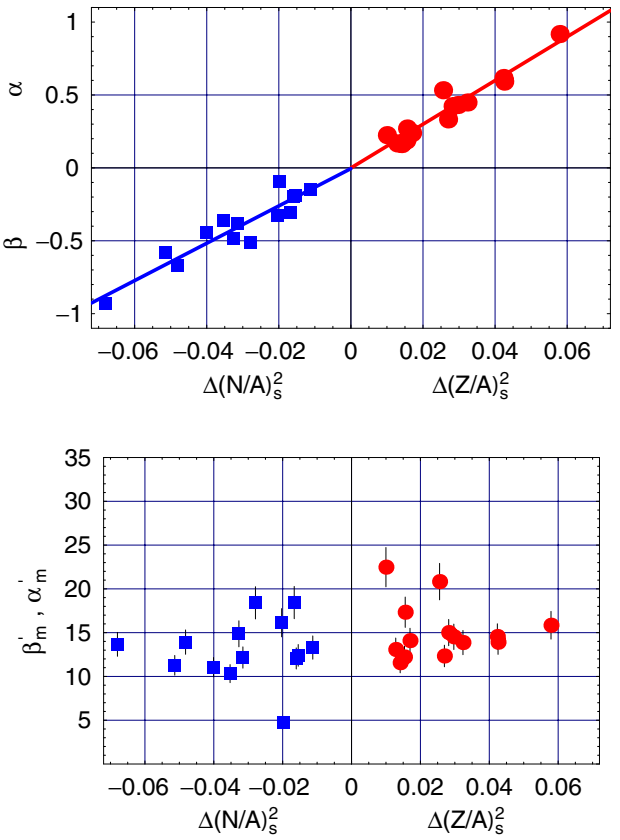

Fig. 10. The isoscaling parameters for 14 combinations of ^{58,60,62,64}Ni and ^{70,76}Ge targets presented in fig. 8 as a function of the coordinates $\Delta(Z/A)^2_s$ and $\Delta(N/A)^2_s$. Upper panel: the isoscaling parameters α (points) and β (boxes) obtained with eq. (1). Lower panel: the reduced isoscaling parameters α'_m (points) and β'_m (boxes) obtained with eqs. (16).

initial projectile-target combination (p+A_t). This approximation does not contradict recent AMD model calculations [14,36] for nucleus-nucleus interactions which predict a linear relationship between the initial asymmetry $(Z/A)^2_{t=0}$ in the dynamical evolution and the corresponding one at $t = 300\,\mathrm{fm}/c$, *i.e.* when the fragments are already produced.

The results shown in the upper panel of fig. 10 confirm the hypothetical factors for analysis in eq. (16). Thus, it was possible to confirm unified isoscaling (see relations (13)) in both the semiempirical and the model-based procedures.

5 Discussion

Our results may be compared with findings of other analyses. The slopes α *versus* $\Delta(Z/A)^2$ found for projectile residues from peripheral collisions of ^{58,64}Ni and ^{136}Xe with targets of Sn, Au, Pb and Th [8] agree astonishingly with our results, whereas α and β derived from the spallation data are only few percents larger. The slope of the isoscaling parameters α *versus* $\Delta(Z/A)^2$ derived from fragments produced in the multifragmentation of ^{58}Ni + ^{58}Ni, ^{58}Fe + ^{58}Ni and ^{58}Fe + ^{58}Fe [37] are about 35% larger than for our corresponding spallation data. Consequently, the isoscaling parameters α obtained from spallation residues are placed in-between the results of the other data sets.

On the other hand, the reduced parameters α'_m and β'_m are rather independent of $\Delta(Z/A)^2_s$ and $\Delta(N/A)^2_s$, respectively, as shown in fig. 10, lower panel. This result again is in agreement with a nearly constant temperature evidenced in fig. 3. However, the temperatures in this figure are given in arbitrary units due to missing proper calibration factors for the used thermometers. But one may try to extract the symmetry term by using isotope temperatures found for light fragments (Z = 2–5) in 1 GeV-proton interactions with targets of ^{58,64}Ni. In this case, from the measured double isotopic yield ratios a temperature $T \sim 4.5$ MeV has been extracted [13]. Using this temperature and the obtained values of α'_m (see lower panel of fig. 10), relation (17) allows roughly to estimate the symmetry energy term to be $C_{sym} \sim 17 \pm 3$ MeV. Although this value deviate from the standard quantity $C_{sym} = 25$ MeV, the following considerations seem to warrant this result.

In recent publications [35,38] the symmetry energy has been calculated in dependence on the excitation energy E_{exc}. The temperature $T \simeq 4.5$ MeV can be converted by the Fermi gas relation $E_{exc} = a \cdot T^2$ (with a level density parameter $a = 10/A$) into an excitation energy $E_{exc} \simeq 2.3\ A$ MeV for disassembling ^{60}Ni. On the other hand, the mean multiplicity of nucleons emitted in 1 GeV proton + ^{58}Ni, ^{60}Ni interactions, leading to a ^{42}Ca residue, provides $E_{exc} \simeq 200$ MeV or $\simeq 3.4\ A$ MeV [31], respectively. The excitation energy is mostly dissipated by sequential emission of light particles in spallation as well as in projectile-fragmentation reactions. Therefore, we refer to symmetry energies found from an analysis of projectile-fragment distributions within a modified abrasion-ablation model [35]. The evaluated parameters of the symmetry energy scatter from $C_{sym} \simeq 10$ MeV to $C_{sym} \simeq 20$ MeV within the interval of excitation energies from 2.3 A MeV to 3.4 A MeV.

However, the evaluation of C_{sym} from isoscaling parameters α and β must be done with caution due to their high sensitivity on $\Delta(Z/A)^2_s$ of the emitting sources. For example, already an uncertainty of ± 1 nucleon in the nucleonic composition of one of the emitting sources falsifies the value of C_{sym} by about $\pm$(10–30)%.

Figures 8 and 10 show that the points scatter from the fit line more at smaller $\Delta(N/Z)_s$ or $\Delta(Z/A)^2_s$. Hence, the preferable combinations to evaluate C_{sym} are combinations with a sufficiently large difference in the nucleonic composition of the emitting sources.

6 Conclusions

In summary, single and double yield ratios of isotopes were analysed to study statistical properties of spallation residues from 1 GeV-proton+nucleus interactions. The yield ratios of adjacent isotopes of these reaction

products meet criteria derived for an equilibrated system described by the grand-canonical approach. It means that a fraction of the order of few percents of the total reaction cross-section undergoes equilibrium. This behaviour is also indicated by the constant isotope temperatures (obtained from double isotope yield ratios) which are nearly the same in a wide range of target masses.

The yield ratios $Y_2(N,Z)/Y_1(N,Z)$ of a specific isotope for arbitrary target pair combinations are found to exhibit isoscaling properties up to $N = 33$ and $Z = 28$. The isoscaling parameters α and β were found to be highly sensitive to the nucleonic composition of the emitting sources. This dependence can be taken into account by the quantity which is either linear in $\Delta(N/Z)_s$ of the fragmenting sources or depends on $\Delta(Z/A)_s^2$ as predicted by several models.

Unified isoscaling for comparative tests of numerous combinations of spallation reactions was proposed whereby the reduced isoscaling parameters α' and β' substitute the former parameters α and β. Without restrictions to the choice of the target pair combinations, the absolute values of the reduced parameters α' and β', both proportional to the reciprocal of the nuclear temperature, were found to be approximately the same. Consequently, one can suppose that all considered spallation products are to be produced at a similar temperature.

The established unified isoscaling is supposed to be used in forthcoming studies to enlighten the nucleonic composition at the break-up of excited nuclei.

The authors are indebted to Dr. L.N. Batist for making available his experimental data. We are very grateful to Prof. M.B. Tsang for stimulating discussions and a careful reading of the manuscript during the early stage of this work. W.N. thanks for financial support during his stay at PNPI Gatchina. Part of this work is supported by the National Science Foundation under Grant Number INT-0218329.

References

1. H.S. Xu *et al.*, Phys. Rev. Lett. **85**, 716 (2000).
2. M.B. Tsang *et al.*, Phys. Rev. Lett. **86**, 5023 (2001).
3. M.B. Tsang *et al.*, Phys. Rev. C **64**, 054615 (2001).
4. W.A. Friedman, Phys. Rev. C **69**, 031601(R) (2004).
5. M. Veselsky, G.A. Souliotis, M. Jandel, Phys. Rev. C **69**, 044607 (2004).
6. M.N. Andronenko, L.N. Andronenko, W. Neubert, PNPI-2541 (2003) unpublished.
7. G.A. Souliotis *et al.*, Phys. Rev. C **68**, 024605 (2003).
8. G.A. Souliotis *et al.*, Phys. Rev. C **73**, 024606 (2006).
9. A.S. Botvina *et al.*, Phys. Rev. C **65**, 044610 (2002).
10. A.S. Botvina, I.N. Mishustin, arXiv:nucl-th/0510081 (2005).
11. W.A. Friedman, Phys. Rev. Lett. **60**, 2125 (1988).
12. A.Y. Abul-Magd, W.A. Friedman, J. Hüfner, Phys. Rev. C **34**, 113 (1986).
13. M.N. Andronenko *et al.*, Eur. Phys. J. A **8**, 9 (2000).
14. A. Ono *et al.*, Phys. Rev. C **68**, 051601 (2003).
15. M.B. Tsang *et al.*, Phys. Rev. C **64**, 041603(R) (2001).
16. J. Adam *et al.*, nucl-ex/0302032 (2003).
17. M. Noguchi *et al.*, Phys. Rev. C **38**, 1811 (1988).
18. L.Ch. Batist *et al.*, LNPI-606 (1980); LNPI-677 (1981); LNPI-746 (1982) unpublished.
19. L.Ch. Batist, PhD Thesis, PNPI, Gatchina, 1988.
20. M.N. Andronenko *et al.*, PNPI-2458 (2001) unpublished; arXiv:nucl-ex/0112014 (2001).
21. M.N. Andronenko, L.N. Andronenko, W. Neubert, Prog. Theor. Phys. (Kyoto), Suppl. **146**, 538 (2002).
22. J. Randrup, S.E. Koonin, Nucl. Phys. A **356**, 223 (1981).
23. R. Wada *et al.*, Phys. Rev. Lett. **58**, 1829 (1987).
24. D. Hahn, H. Stöcker., Nucl. Phys. A **476**, 718 (1988).
25. H.W. Barz *et al.*, Phys. Lett. B **211**, 10 (1988).
26. W. Neubert *et al.*, Annual Report FZR 93-10 (1992) unpublished.
27. J. Pochodzalla, W. Trautmann, GSI Darmstadt 2000-27, unpublished.
28. L.N. Andronenko *et al.*, in *Proceedings of the 7th International Conference on Clustering Aspects of Nuclear Structure and Dynamics, Rab, 1999*, edited by Z. Basrak *et al.* (World Scientific, Singapore, 2000) p. 370.
29. S. Albergo *et al.*, Nuovo Cimento **89**, 1 (1985).
30. V.S. Barashenkov, V.D. Toneev, *Interactions of High-energy Particles and Atomic Nuclei with Nuclei* (Atomizdat, Moscow, 1972) in Russian.
31. E.N. Volnin, in *Proceedings of the Symposium on Nucleon-Nucleon and Hadron-Nucleus Interactions at Intermediate Energies, Gatchina, April 23-25, 1984*, edited by A. Moskalev *et al.* (Academy of Science of the USSR, Leningrad Nuclear Physics Institute Publishing Office, Leningrad, 1984).
32. M.N. Andronenko, L.N. Andronenko, W. Neubert, PNPI-2540 (2003) unpublished.
33. M.B. Tsang *et al.*, Phys. Rev. C **66**, 044618 (2002).
34. W.A. Friedman, Phys. Rev. Lett. **60**, 2125 (1988); Phys. Rev. C **42**, 667 (1990).
35. D.Q. Fang *et al.*, arXiv:nucl-th/0601067 (2006).
36. A. Ono *et al.*, Nucl. Phys. A **738**, 308 (2004).
37. D.V. Shetty *et al.*, Phys. Rev. C **70**, 011601 (2004).
38. W. Trautmann *et al.*, arXiv:nucl-ex/0603027 (2006).